SPS2022
A.H.C. Ng et al. (Eds.)

doi:10.3233/ATDE220173

Acoustic Diagnostic of Laser Powder Bed Fusion Processes

IVAN ZHIRNOV[a,1] and DEAN KOUPRIANOFF[b]
[a] *Karlstad University, Sweden*
[b] *Central University of Technology, South Africa*

Abstract. Online monitoring of Laser Powder Bed Fusion is critical to advance the technology and its applications. Many studies have shown that the acoustic signal from the laser powder bed fusion process contains a large amount of information about the process condition. In this research, we used an acoustic system for the in-situ characterization of a wide variety of different single-track geometries. The internal acoustic system includes a microphone and accelerometer. The melting mode, cross-sectional shape and dimensions of Ti6Al4V single tracks at different process parameters are presented. We have established a correlation between track geometry, internal defects and acoustic signals. The parameters are varied and tested against the acoustic frequency measurements to determine the sensitivity. We determined the patterns of signal behaviour in the event of anomalies (spatter, balling, pores, undercut). The characteristic features of the process are traced to a commercial machine. Well described dataset with correlated monitoring data and signal tracks properties obtained and can be used for building classification model and quality prediction. All this is aimed at creating a database of experimental data that will be a key for LPBF digitalization and control, allowing real-time control of the process to optimize part quality and, more importantly, help with decision-making algorithms.

Keywords. Laser powder bed fusion, acoustic diagnostic, process monitoring, frequency domain features, data processing.

1. Introduction

Due to a wide range of scientific research, it has become known that Laser Powder Bed Fusion (LPBF) is multifactorial [1]. Many critical flaws can occur without changing the characteristics of the upper layer, for example, subsurface cracks and pores [2]. Part quality and certification are becoming increasingly crucial for additive manufacturing, especially for industrial aerospace and other safety-critical applications. Online monitoring is challenging since LPBF is sensitive to many small-scale variables, which cannot be easily tracked and measured [3,4]. Therefore online monitoring has become the leading research area with large scale projects such as 'Real-Time Monitoring and Control of Additive Manufacturing Processes' at NIST in the USA [5].

Most commercial LPBF machines have implemented monitoring systems based on optical sensors such as cameras and photodiodes [6]. The building process can take up to several hours or days; therefore, any monitoring system is faced with the challenge to analyze an incredible amount of data. A high-speed imaging system can result in large

[1] Corresponding Author, Ivan.Zhirnov@kau.se

amounts of data, up to 75.1 GB of images every second [7]. In contrast, recording with a 24bit microphone at 100 000 samples per second would result in 0.3MB/s. Hall [8] published a world patent for using gas borne acoustic emission (AE) for LPBF online monitoring in 2016 and 2017. Some initial results for applying this method in a commercial machine was reported [9]. At the same time, structured based AE was reported as early as 2016 [10], and two years earlier, a more conventional structural ultrasonic testing method based on sending and receiving waves through the part as it is being built was investigated [11,12].

Many developments aim to process big data produced by optical monitoring systems[13] using artificial intelligence and, more specifically, AE [14, 15]. Machine learning is used to find the dependencies between the input parameters and sensor data to determine the quality of the final part. Another development for gas borne AE for LPBF is using an optical microphone [16,17]. This allows for a much greater frequency range but at an increased cost and complexity. Ito et al. [18] measured structure AE for frequencies above 50kHz and found that they could identify the position of a single track using two sensors.

Although AE monitoring for LPBF has been proven to give valuable information, much work is needed for the technology to be established/implemented. In a review of online monitoring, Yadav et al. [6] concluded that it is still in infancy. None of the online monitoring methods can cover all types of different defects [19].

For gas borne AE systems that do not rely on artificial intelligence, data sizes analyzed using digital signal processing is limited due to the incredible amount of time it takes to extract and analyze signals, not to mention preparing the micrographs and analyzing the corresponding physical tracks. Therefore, this paper aims to present quality data of gas, and structure-borne AE features with greater statistical significance for a wide range of process variables. This is done by carefully considering variables such as the layer thickness controlled by grooved substrates and analyzing a more significant amount of data. At the same time, keeping industrialization in mind, a commercial machine with a simple, inexpensive gas borne AE and contact piezoelectric accelerometer setup is used.

2. Methodology

The experiment consists of two plates on which single tracks are produced using different parameters while measuring the sound and vibrations. Two plates were designed; the first; used to measure a wide range of laser parameters, i.e., laser power and scanning speed. The second plate measures slight changes in layer thickness directly related to the amount of material involved.

The experiments were done in a commercial Renishaw AM400 LPBF machine equipped with a reduced build volume module using Ti6Al4V powder and substrates. While careful consideration not to disrupt the machine's regular operation, a microphone, accelerometer, and camera were fitted inside the chamber, as shown in Figure 1.

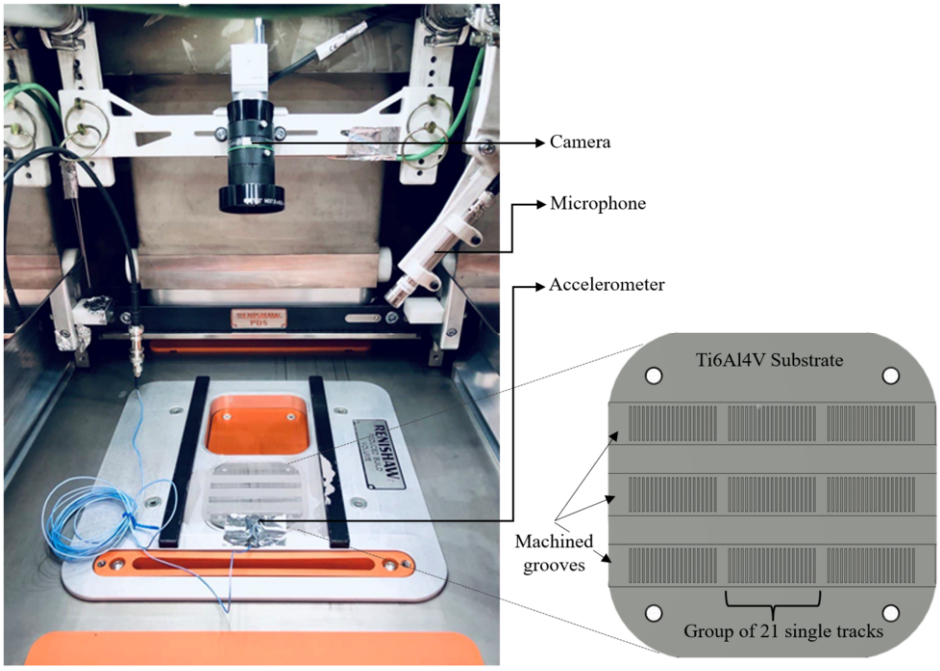

Figure 1: Renishaw 400 chamber with acoustic sensors, camera and grooved substrate

During this experiment, one of the main tasks was to create a large variety of signals that could correspond to various geometries of the single track. The substrates were machined with grooves varying in depth to accurately measure the influence of layer thickness on acoustic emission. This allows better control over the amount of material involved in the process.

The machine is equipped with a 1070 nm laser with a 65 µm spot size and a point-by-point laser exposure methodology. TI6Al4V (ELI) gas atomized powder with the following chemical composition was used: Ti – balance, Al – 6,35%, V – 3,73%, Fe – 0,17% (weight %). The equivalent diameters (by volume) of the powder particles were d10 = 12 µm, d50 = 21 µm and d90 = 31 µm.

2.1. Plate 1 Laser parameters

The different laser parameters for both plates can be seen in Table 1. For Plate 1, the laser parameters were varied in such a manner to measure the influence of specific changes; For sets 1-7, the energy density was kept at approximately the same level by changing both the laser power and speed. For sets 8,9,12,15, and 16, the laser power was constant, only varying the scanning speed by ±5 and ±10%. For sets 10,11,12,13,14, the scanning speed was constant, the laser power varying by ±5 and ±10%.

Table 1. Laser parameters for Plate 1 and 2.

Set	Laser Power (W)	Scanning speed(m/s)	Energy density (j/m)	Plate 1 30 & 50µm	Plate 2 50,60,70,80,90 & 100µm
1	400	1,00	400	x	
2	375	0,93	403	x	
3	350	0,87	403	x	
4	325	0,81	402	x	
5	300	0,75	401	x	
6	275	0,68	402	x	
7	250	0,63	400	x	x
8	280	1,43	196	x	
9	280	1,37	205	x	
10	308	1,30	237	x	
11	294	1,30	226	x	
12	280	1,30	215	x	x
13	266	1,30	205	x	
14	252	1,30	194	x	
15	280	1,24	227	x	
16	280	1,17	239	x	
17	100	1,20	83	x	
18	170	0,66	259	x	
19	170	0,45	375	x	
20	170	0,35	492	x	
21	170	0,28	609	x	

For sets 17-21, extreme deviation from optimal process parameters was chosen. These would lead to the deep keyhole, balling and irregular single tracks. 8mm single tracks were produced for each parameter set, three tracks at 30µm and six at 50 µm. Each tracks' dimensions were measured from the top and at two cross-sections resulting in 18 measurements each.

2.2. Plate 2 Powder increments

After analysing Plate 1, only two laser parameters (Table 1) were selected for the layer thickness variation (Table 2). The powder layer thickness was changed in 10 µm increments, as shown in Table 2. Each track was repeated 11 times, and 22 cross-sections were analysed for each laser parameter at each layer thickness.

Table 2. Layer thickness parameters

Thickness (µm)	0	30	50	60	70	80	90	100
Plate 1		x	x					
Plate 2	x		x	x	x	x	x	x

2.3. Data acquisition and processing

The sound and vibrations emitted from the process were recorded with a microphone and accelerometer, each sampled at 102.4 kHz and taking into account the Nyquist frequency, we obtained a frequency range from 0 to 51.2 kHz. Microphone – PCB 378B02, sensitivity 50 mV/Pa, accelerometer – PCB 352A21, sensitivity 10 mV/g, hardware – NI CompactDAQ-9185 with sound and vibration input module NI-9250 were

used for monitoring. The data was filtered using a 1kHz high pass filter, and each set was cut and measured using the following six features;

- mean frequency; simply the product of the frequency and its intensity divided by the total spectrum intensity
- peak frequency; the frequency with the maximum intensity
- power spectral density (calculated for 10kHz bands)
- spectral centroid (SC); centre of mass of the spectrum
- root mean squared (RMS); calculated by the square root of the arithmetic mean of the squares and indicates the energy in the signal or represents loudness
- zero-crossing rate (ZCR); an indicator that reflects the fluctuations of a curve in a given time interval (smoothness).

3. Results and Discussion

After processing, the cross-sections of the tracks were analysed in two places. This variety allowed us to get a relatively large range of possible track shapes. From the top view, tracks were classified into four groups: irregular, balling, continuous and spatter or satellites, and two groups of internal defects such as pores and undercut (Figure. 2).

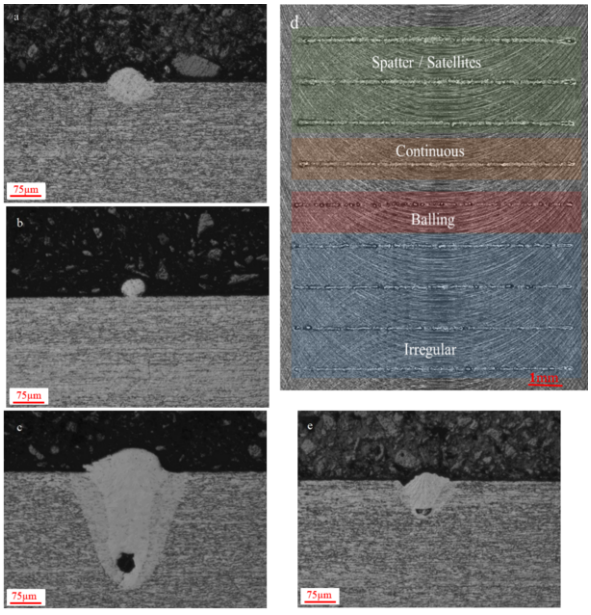

Figure 2: Top of 4 different shapes (d) and cross-sectional views of the single tracks; a - continuous, b - balling, c - pore, e - pore and undercut.

As a result, we obtained 189 tracks from plate 1 and 152 tracks from plate 2, which resulted in 680 measurements of the molten pool geometry. The plot on the top of Figure 3 shows the correlation between the linear energy density (laser power/scanning speed) and the aspect ratio. As expected, more energy leads to a bigger melt pool. Also, here some data clustering in the shape of the track for the aspect ratio and energy density is

present. The dataset contains a variety of tracks with pores and undercuts and tracks free from defects.

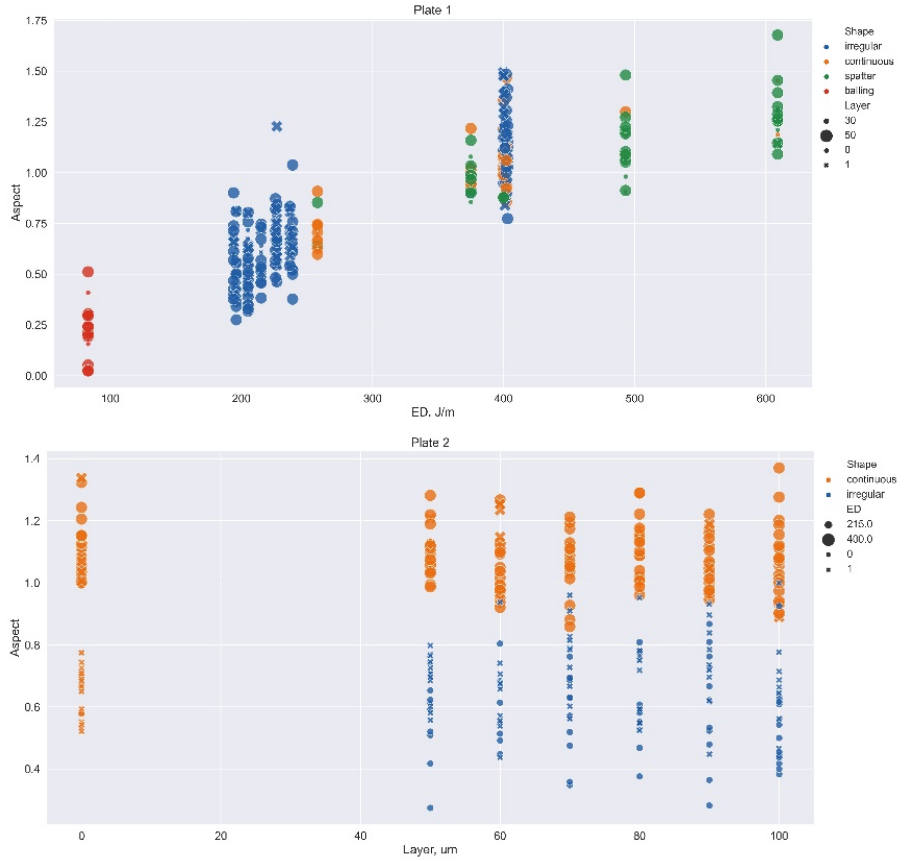

Figure 3: Aspect ratio vs energy density (Plate 1) and Aspect ratio vs layer thickness (Plate 2). Style of markers represent internal defect; 0 – defect-free, 1 – pore or undercut.

Both sensors showed sensitivity even to the minor changes in process parameters. Many studies have shown that an acoustic signal carries a relatively large time and frequency domain information. The average time per track for the various process parameters was about 10ms, meaning that, on average, 1000 points were recorded per track. That amount turned out to be enough to recognise differences in various track shapes and internal defects, as shown in Figure 4. The Short-Time Fourier Transform (STFT) calculates the frequency over time. It is represented on a plot of frequency against time, with the colour indicating intensity. Four different tracks for both the accelerometer and microphone recordings are shown to have apparent differences. Many studies use raw acoustic signals as an input for machine learning algorithms for clustering, classification and other implementations [20].

To reduce the amount of data, speed up the computation and possibly increase the accuracy, we focused on the search for signal properties that correlate with the properties of the track. In the future, it is planned to use a similar approach, but applying for

complex build and analysing the signal by layers. The point of this work is a combination of a microphone and an accelerometer. Recent studies have shown the effectiveness of using a microphone in the monitoring process of LPBF, but also its disadvantages. By supplementing the acoustic signal of the microphone with measurements of the vibration from the melt pool using an accelerometer installed directly on the surface of the laser interaction with the material, we were able to increase the number of process signatures for establishing correlations.

The images obtained after STFT can be used to classify or cluster data. The difference in the behaviour of frequencies when changing the process parameters is immediately visible. At this stage, we do not intend to use machine learning algorithms, so we investigated only the numerical characteristics of the signal.

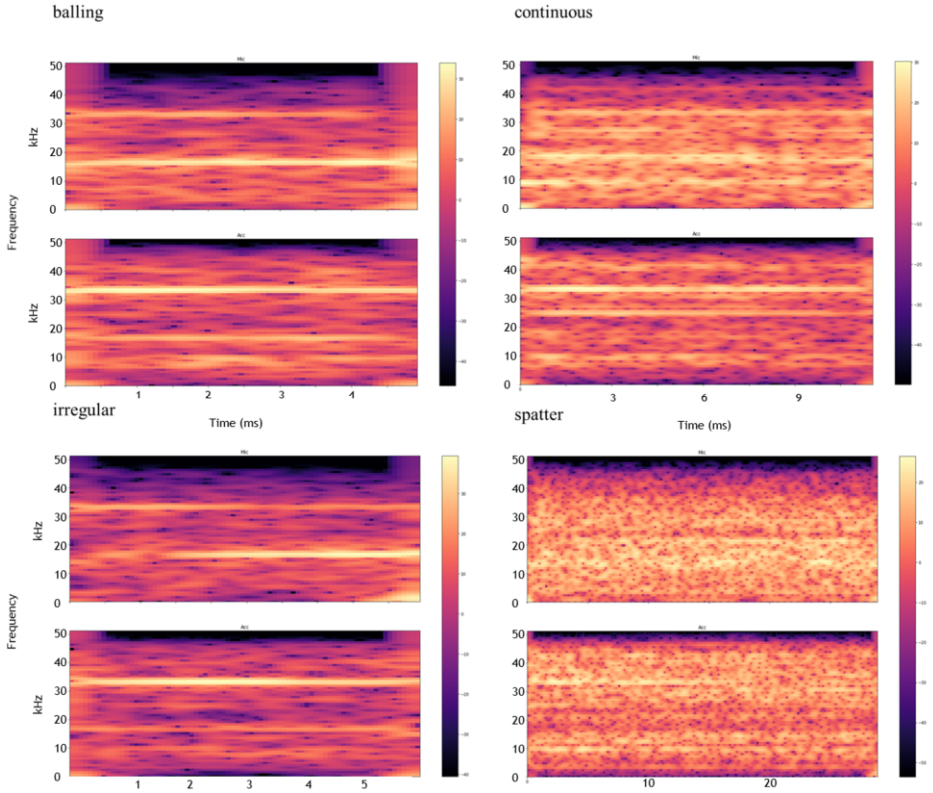

Figure 4: Typical STFT spectrograms for different energy densities: balling – 83, continuous – 400, irregular – 215, spatter – 609 J/m. Layer thickness 50 um. For each energy density, the microphone is at the top and the accelerometer bottom.

The six signal features described in section 2.3 have been calculated for each track. Since each characteristic is distributed over time, we took the median and standard deviation for each track for comparison reasons. The combination of all measurements and recordings from the microphone and accelerometer is shown in Figure 5. It was observed that the spectral centroid of the microphone practically remains at 17 kHz, while the data from the accelerometer show that for the "unstable" modes (balling and spatter), the average frequency is much higher than for stable tracks (Figure 5). Also, tracks with irregular geometry have the most extensive deviations. The presence of pores

and undercuts in stable tracks can be attributed to a slight shift of the average frequency towards lower frequencies. A similar trend is observed for the peak frequency values. This trend can be traced quite clearly if we use the spectral centroid. The RMS is very sensitive to the presence of internal defects. For almost all track shapes, the scatter of the data increases for undercut and the average RMS value increases in the presence of pores. This is quite logical since this parameter is usually responsible for the loudness of the signal. ZCR represents the "smoothness" of the signal, which is typical for stable continuous tracks without internal defects. For the current experiment, these two are the most representative signal features.

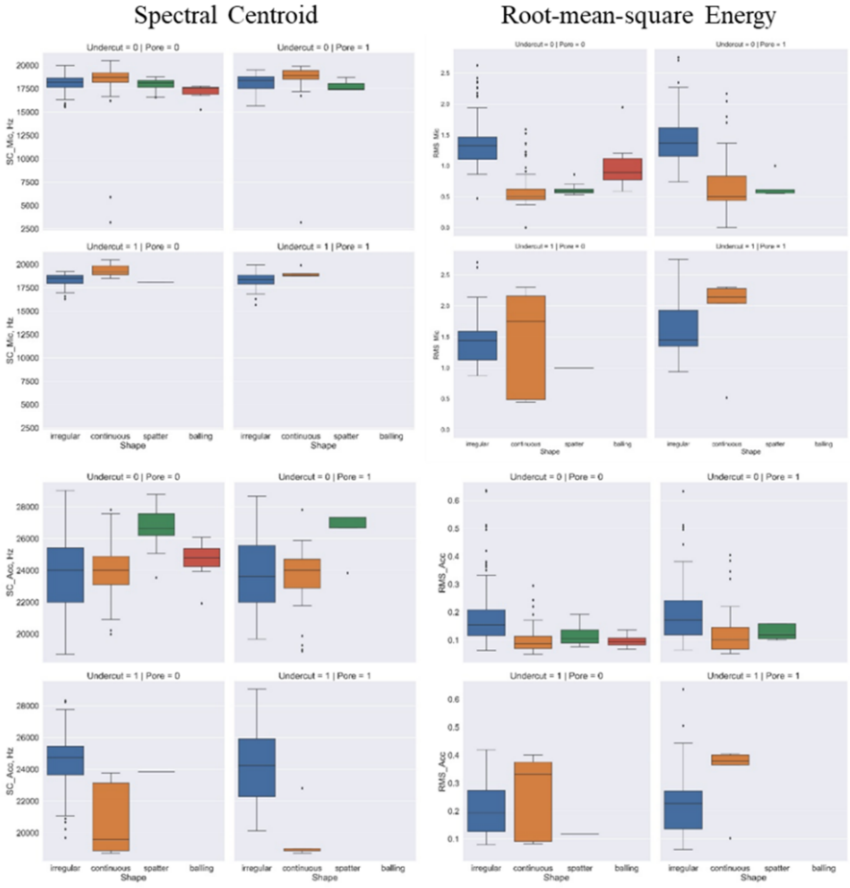

Figure 5: Boxplot for Spectral centroid and RMS of all tracks vs shape types. The box represents data between 25th to 75th percentile, with the line being the median and dots outliers.

Even considering the multiple repetitions, we face high volatility of signals, one of the reasons being the transient oscillatory motion of the melt pool [21]. This again proves that the laser powder bed fusion process is stochastic and requires constant monitoring and control. A more significant number of deviations are levelled by subsequent layers due to the transfer, but research shows that there is still a process of accumulation and the effect of stochasticity. This can also be seen in research employing rescanning before

depositing the next layer [2]. The process requires in-line process adjustment, which will be more efficient than using a constant energy input.

For the entire dataset, we decided to check the Pearson coefficient correlation matrix (Figure 6). This calculation is more appropriate for linear relationships such as energy density and penetration depth. Nevertheless, some dependencies are present, for example, in the presence of internal defects, bandwidth and RMS for both types of sensors. The number of correlation coefficients from the data of the second plate shows significant sensitivity of the signal features to the layer thickness shift. This might be valuable for the detection of a lack of powder during the build. Correlations are present, and they rather have a nonlinear and multiparametric format, which requires complex models with regularisation of the given data, a more significant amount of data, and a combination of signal features. Complete data package including a spectrogram, process parameters, multiple quantitative characteristics of the signal should be acquired and fused for input to a complex algorithm.

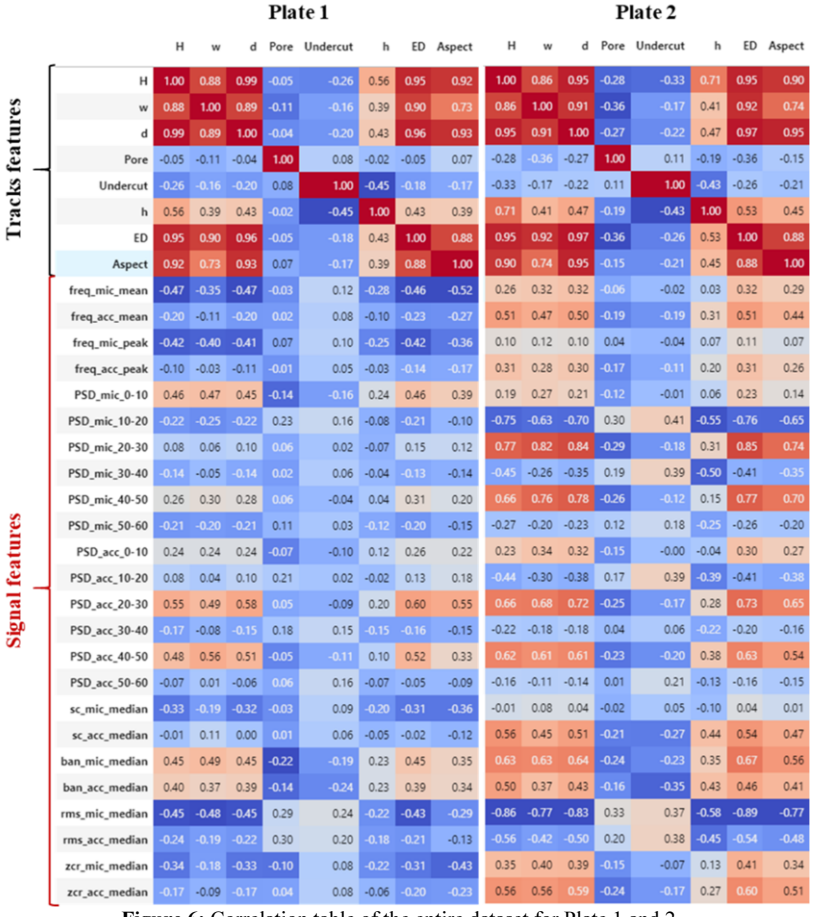

Figure 6: Correlation table of the entire dataset for Plate 1 and 2.

4. Conclusion

In this research, we have demonstrated that a simple monitoring system composed of a microphone and accelerometer easily installed in the commercial machine allows us to determine the patterns of formation of laser melting anomalies such as spatter, balling, pores, and undercut during the laser powder bed fusion of single tracks.

Obtained results showed that the combination of two acoustic sensors provides different acoustic signatures from the melt pool. The shift of the values of different acoustic signal features from both sensors relative to the melt pool geometry is statistically distinguishable.

A diverse labelled dataset for single tracks and related acoustic features was obtained. Different track features (shape, porosity, undercut) were linked to the acoustic signals. The correlation matrix from both plates shows this link.

The current dataset will be expanded and used for the quality prediction model. Any of these methods can be used as part of an emergency stop of the entire process. We recognise that data from the acoustic emissions contain a large amount of unique information about the process, and when in combination with an optical monitoring system, diversifies the data for machine learning models.

5. Acknowledgements

The authors also want to thank the Swedish Agency for Economic and Regional Growth, Grant No20201144, ATLAB - additive manufacturing laboratory at Karlstad University, Centre for Rapid Prototyping, the South African Collaborative Program in Additive Manufacturing (CPAM) and Manufacturing and Region Värmland for financial support. This research was co-financed by KK-Foundation project “Advanced Materials for High Performance Products–AMHIPP” (no. 20190033; Stockholm, Sweden).

References

[1] Spears TG & Gold SA. In-process sensing in selective laser melting (SLM) additive manufacturing. Integr. Mater. Manuf. Innov, 2016 Feb 5, 16–40. https://doi.org/10.1186/s40192-016-0045-4.

[2] Yadroitsev I, Krakhmalev P, Yadroitsava I. Hierarchical design principles of selective laser melting for high quality metallic objects. Additive Manufacturing, 2015 Jul; p. 75–56. https://doi.org/10.1016/j.addma.2014.12.007.

[3] Grasso M, Colosimo BM, Slattery K, MacDonald E. Process monitoring of laser powder bed fusion. In Additive Manufacturing Materials and Technologies, Fundamentals of Laser Powder Bed Fusion of Metals, 2021 11; p 301-326, Elsevier. https://doi.org/10.1016/B978-0-12-824090-8.00012-3.

[4] Lu QY and Wong CH. Additive manufacturing process monitoring and control by non-destructive testing techniques: challenges and in-process monitoring. Virtual Phys. Prototyp, 2018 13, p. 39–48. https://doi.org/10.1080/17452759.2017.1351201.

[5] NIST. Qualification for additive manufacturing materials, processes and parts (Online) 2020, Available from: https://www.nist.gov/programs-projects/real-time-monitoring-and-control-additive-manufacturing-processes (Accessed on 27 October, 2021).

[6] Yadav P, Rigo O, Arvieu C, Le Guen E, Lacoste E. In situ monitoring systems of the SLM process: On the need to develop machine learning models for data processing. Crystals, 2020 10; p. 524. https://doi.org/10.3390/cryst10060524.

[7] Berumen S, Bechmann F, Lindner S, Kruth JP, Craeghs T. Quality control of laser- and powder bed-based Additive Manufacturing (AM) technologies. Physics Procedia, 2010 5, p. 617–622.

[8] Hall, LD. WO2016198885A1 - Additive Manufacturing Apparatus and Method - Google Patents, 2016. Available at: https://patents.google.com/patent/WO2016198885A1/en (accessed June 17, 2020).

[9] Kouprianoff D, Luwes N, Newby E, Yadroitsava I, Yadroitsev I. On-line monitoring of laser powder bed fusion by acoustic emission: Acoustic emission for inspection of single tracks under different powder layer thickness, 2017 Pattern recognition association of South Africa and robotics and mechatronics international conference (PRASA-RobMech), 2017; p. 203–207 http://dx.doi.org/10.1109/RoboMech.2017.8261148

[10] Fisher KA, Candy JV, Guss G, Mathews JM. Evaluating acoustic emission signals as an in situ process monitoring technique for selective laser melting (SLM) (No. LLNL-TR-706659). Lawrence Livermore National Laboratory (LLNL), 2016, Livermore, CA.

[11] Rieder H, Dillhöfer A, Spies M, Bamberg J, Hess T. Online Monitoring of Additive Manufacturing Processes Using Ultrasound, in: Proceedings of the 11th European Conference on Non-Destructive Testing, 2014; p. 2194–2201.

[12] Slotwinski JA, Garboczi EJ, Hebenstreit KM. Porosity measurements and analysis for metal additive manufacturing process control. Journal of Research of the National Institute of Standards and Technology, 2014 119; p. 494. https://doi.org/10.6028/jres.119.019.

[13] Zouhri W, Dantan JY, Häfner B, Eschner N, Homri L, Lanza G, Theile O, Schäfer M. Optical process monitoring for Laser-Powder Bed Fusion (L-PBF). CIRP Journal of Manufacturing Science and Technology, 2020 Nov; 31, p. 607-617 https://doi.org/10.1016/j.cirpj.2020.09.001.

[14] Ye D, Hong GS, Zhang Y, Zhu K, Fuh JYH. Defect detection in selective laser melting technology by acoustic signals with deep belief networks. Int J Adv Manuf Technol, 2018 96, p. 2791–2801. https://doi.org/10.1007/s00170-018-1728-0.

[15] Eschner N, Weiser L, Häfner B, Lanza G. Classification of specimen density in Laser Powder Bed Fusion (L-PBF) using in-process structure-borne acoustic process emissions. Additive Manufacturing, 2020 Aug; 34, 101324 https://doi.org/10.1016/j.addma.2020.101324.

[16] Prieto C, Fernandez R, Gonzalez C, Diez M, Arias J, Sommerhuber R, Lücking F. In situ process monitoring by optical microphone for crack detection in Laser Metal Deposition applications. In 11th CIRP Conference on Photonic Technologies [LANE 2020], 2020.

[17] Gutknecht K, Cloots M, Sommerhuber R, Wegener K. Mutual comparison of acoustic, pyrometric and thermographic laser powder bed fusion monitoring. Materials & Design, 2021 Nov; 210. https://doi.org/10.1016/j.matdes.2021.110036.

[18] Ito K, Kusano M, Demura M, Watanabe M. Detection and location of micro defects during selective laser melting by wireless acoustic emission measurement. Additive Manufacturing, 2021 April; 40 101915. https://doi.org/10.1016/j.addma.2021.101915.

[19] Malekipour E & El-Mounayri H. Common defects and contributing parameters in powder bed fusion AM process and their classification for online monitoring and control: a review. Int J Adv Manuf Technol 2018 March 95; p. 527–550. https://doi.org/10.1007/s00170-017-1172-6.

[20] C. Wang, X.P. Tan, S.B. Tor, C.S. Lim. Machine learning in additive manufacturing: state-of-the-art and perspectives. In Add. Manuf., 36 (2020), p. 101538. https://doi.org/10.1016/j.addma.2020.101538.

[21] Khairallah SA, Sun T, Simonds BJ. Onset of periodic oscillations as a precursor of a transition to pore-generating turbulence in laser melting. Additive Manufacturing Letters, 2021 Dec; 100002. https://doi.org/10.1016/j.addlet.2021.100002.